8-11-2015

Phytoplankton-Bacterial Interactions Mediate Micronutrient Colimitation at the Coastal Antarctic Sea Ice Edge

Erin M. Bertrand

John P. McCrow

Ahmed Moustafa

Hong Zheng

Jeffrey B. McQuaid

See next page for additional authors

Citation/Publisher Attribution

Bertrand EM, McCrow JP, Moustafa A, Zheng H, McQuaid JB, Delmont TO, Post AF, Sipler RE, Spackeen JL, Xu K, Bronk DA, Hutchins DA, Allen AE. (2015). "Phytoplankton-bacterial interactions mediate micronutrient colimitation at the coastal Antarctic sea ice edge." Proceedings of the National Academy of Sciences, 112(32), 9938-9943.

Available at: http://dx.doi.org/10.1073/pnas.1501615112

Phytoplankton–bacterial interactions mediate micronutrient colimitation at the coastal Antarctic sea ice edge

Erin M. Bertrand[a,b,1], John P. McCrow[a], Ahmed Moustafa[a,b,c], Hong Zheng[a], Jeffrey B. McQuaid[a,b], Tom O. Delmont[d], Anton F. Post[e], Rachel E. Sipler[f], Jenna L. Spackeen[f], Kai Xu[g], Deborah A. Bronk[f], David A. Hutchins[g], and Andrew E. Allen[a,b,2]

[a]Microbial and Environmental Genomics, J. Craig Venter Institute, La Jolla, CA 92037; [b]Integrative Oceanography Division, Scripps Institution of Oceanography, University of California, San Diego, La Jolla, CA 92037; [c]Department of Biology and Biotechnology Graduate Program, American University in Cairo, Cairo, Egypt 11835; [d]Josephine Bay Paul Center, Marine Biological Laboratory, Woods Hole, MA 02543; [e]Graduate School of Oceanography, University of Rhode Island, Narragansett, RI 02882; [f]Department of Physical Sciences, Virginia Institute of Marine Science, Gloucester Point, VA 23062; and [g]Marine and Environmental Biology, Department of Biological Sciences, University of Southern California, Los Angeles, CA 90089

Edited by David M. Karl, University of Hawaii, Honolulu, HI, and approved July 2, 2015 (received for review January 25, 2015)

Southern Ocean primary productivity plays a key role in global ocean biogeochemistry and climate. At the Southern Ocean sea ice edge in coastal McMurdo Sound, we observed simultaneous cobalamin and iron limitation of surface water phytoplankton communities in late Austral summer. Cobalamin is produced only by bacteria and archaea, suggesting phytoplankton–bacterial interactions must play a role in this limitation. To characterize these interactions and investigate the molecular basis of multiple nutrient limitation, we examined transitions in global gene expression over short time scales, induced by shifts in micronutrient availability. Diatoms, the dominant primary producers, exhibited transcriptional patterns indicative of co-occurring iron and cobalamin deprivation. The major contributor to cobalamin biosynthesis gene expression was a gammaproteobacterial population, *Oceanospirillaceae* ASP10-02a. This group also contributed significantly to metagenomic cobalamin biosynthesis gene abundance throughout Southern Ocean surface waters. *Oceanospirillaceae* ASP10-02a displayed elevated expression of organic matter acquisition and cell surface attachment-related genes, consistent with a mutualistic relationship in which they are dependent on phytoplankton growth to fuel cobalamin production. Separate bacterial groups, including *Methylophaga*, appeared to rely on phytoplankton for carbon and energy sources, but displayed gene expression patterns consistent with iron and cobalamin deprivation. This suggests they also compete with phytoplankton and are important cobalamin consumers. Expression patterns of siderophore- related genes offer evidence for bacterial influences on iron availability as well. The nature and degree of this episodic colimitation appear to be mediated by a series of phytoplankton–bacterial interactions in both positive and negative feedback loops.

colimitation | Southern Ocean primary productivity | metatranscriptomics | phytoplankton–bacterial interactions | cobalamin

Primary productivity and community composition in the Southern Ocean play key roles in global change (1, 2). The coastal Southern Ocean, particularly its shelf and marginal ice zones, is highly productive, with mean rates approaching 300–450 mg C $m^{-2}{\cdot}d^{-1}$ (3). As such, identifying factors controlling phytoplankton growth in these regions is essential for understanding the ocean's role in past, present, and future biogeochemical cycles. Although irradiance, temperature, and iron availability are often considered to be the primary drivers of Southern Ocean productivity (1, 4), cobalamin (vitamin B_{12}) availability has also been shown to play a role (5, 6). Cobalamin is produced only by select bacteria and archaea and is required by most eukaryotic phytoplankton, as well as many bacteria that do not produce the vitamin (7). Cobalamin is used for a range of functions, including methionine biosynthesis and one-carbon metabolism. Importantly, phytoplankton that are able to grow without cobalamin preferentially use it when available; growth without the vitamin occurs at a metabolic cost via use of an alternative methionine synthase enzyme (MetE), rather than the more efficient, cobalamin-requiring version (MetH) (8). The presence of *metE* in phytoplankton genomes does not follow phylogenetic or obvious biogeographical lines; for instance, there are examples of both coastal and open ocean diatoms that require B_{12} absolutely, and some that use it facultatively (7).

Given the short residence time of the vitamin in productive, sunlit surface waters (on the order of hours to days; *SI Appendix*), it is likely that locally produced cobalamin is a predominant source of the vitamin to phytoplankton. *Thaumarchaeota* and cyanobacteria are hypothesized to be major contributors to oceanic cobalamin biosynthesis (9, 10). In the coastal Antarctic

Significance

The coastal Southern Ocean is a critical climate system component and home to high rates of photosynthesis. Here we show that cobalamin (vitamin B_{12}) and iron availability can simultaneously limit phytoplankton growth in late Austral summer coastal Antarctic sea ice edge communities. Unlike other growth-limiting nutrients, the sole cobalamin source is production by bacteria and archaea. By identifying microbial gene expression changes in response to altered micronutrient availability, we describe the molecular underpinnings of limitation by both cobalamin and iron and offer evidence that this limitation is driven by multiple delicately balanced phytoplankton–bacterial interactions. These results support a growing body of research suggesting that relationships between bacteria and phytoplankton are key to understanding controls on marine primary productivity.

Author contributions: E.M.B. and A.E.A. designed research; E.M.B., H.Z., J.B.M., R.E.S., J.L.S., K.X., D.A.B., and D.A.H. performed research; T.O.D. and A.F.P. contributed new reagents/analytic tools; E.M.B., J.P.M., and A.M. analyzed data; and E.M.B., J.P.M., and A.E.A. wrote the paper.

The authors declare no conflict of interest.

This article is a PNAS Direct Submission.

Freely available online through the PNAS open access option.

Data deposition: The data reported in this paper have been deposited in the NCBI sequence read archive (BioProject accession no. PRJNA281813; BioSample accession nos. SAMN03565520–SAMN03565531). Assembled contigs, predicted peptides, annotation, and transcript abundance data for this study can be found at https://scripps.ucsd.edu/labs/aallen/data/.

[1]Present address: Department of Biology, Dalhousie University, Halifax NS, Canada B3H 4R2.

[2]To whom correspondence should be addressed. Email: aallen@jcvi.org.

This article contains supporting information online at www.pnas.org/lookup/suppl/doi:10.1073/pnas.1501615112/-/DCSupplemental.

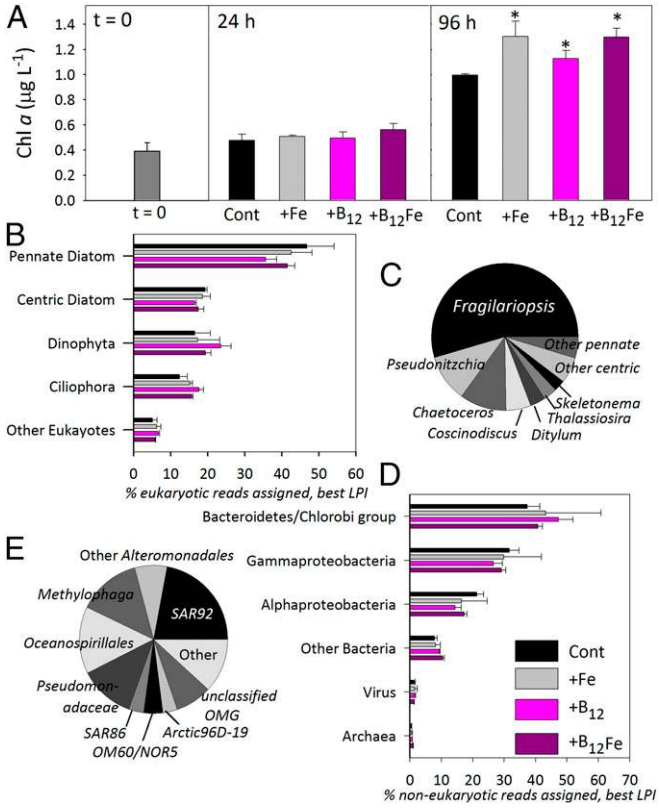

Fig. 1. (*A*) Chl *a* concentrations at 0, 24, and 96 h after micronutrient additions on January 16, 2013, at the McMurdo Sound sea ice edge (*SI Appendix*, Fig. S1). Bars are means of triplicate treatments; error bars are 1 SD about the mean. Significant differences (*t test $P < 0.05$; treatment vs. control) were observed in Chl *a* by 96 h. Upon RNA sequencing after 24 h, no significant differences in mRNA contribution from major taxonomic groups were identified (*B* and *D*). Reads mapping to ORFs with LPI > 0.8 (18) were included. (*C* and *E*) Percentage of reads assigned to diatom and gammaproteobacterial taxa.

Southern Ocean, cyanobacteria are scarce (11), and *Thaumarchaeota* appear to be important, in terms of abundance and contribution to cobalamin biosynthesis proteins, only in winter and springtime (12, 13). Although seasonal trends in Southern Ocean cobalamin concentrations have yet to be investigated, these biogeographic data suggest that Austral summer Southern Ocean cobalamin production may be low relative to other seasons and locations. Indeed, cobalamin limitation has been observed in mid to late summer in the Ross Sea, but was absent in springtime (14). This leads to the hypothesis that reduced cobalamin supply in summer, along with enhanced demand by blooming diatoms, results in possible cobalamin limitation or cobalamin and iron colimitation of primary production. Despite hints that the microbial source of cobalamin during this summertime period may be gammaproteobacterial (15), it has remained uncharacterized to date, rendering inquiry into interactions between microbial sources and sinks of the vitamin difficult. Although instances of mutualistic cobalamin-based interactions between bacteria and algal laboratory cultures have been identified (16), little is known about microbial dynamics surrounding cobalamin production and exchange in the field.

Within McMurdo Sound, which connects the Ross Sea of the Southern Ocean with the McMurdo ice shelf, primary production rates can reach upward of 2 gC $m^{-2}{\cdot}d^{-1}$, with most annual production occurring between December and January (17). Because this area is highly influenced by coastal processes, it has generally been assumed that productivity in the region is not iron-limited (4). However, we show here that at the sea ice edge, McMurdo Sound primary production was both iron- and cobalamin-limited in mid-January 2013, as well as 2015 (Fig. 1; *SI Appendix*, Fig. S1). By examining co-occurring changes in bacterial and phytoplankton transcriptional profiles in response to micronutrient manipulation during this colimited period, we identify specific bacterial and phytoplankton processes that contribute to cobalamin limitation and its relationship to iron dynamics in this key marine region.

Results and Discussion

In a late summer McMurdo Sound community (Fig. 1; *SI Appendix*, Fig. S1 and Table S1), cobalamin and iron addition each independently enhanced chlorophyll *a* (Chl *a*) production, indicating that phytoplankton growth was simultaneously limited by availability of these two micronutrients. The difference in chlorophyll concentrations in the control treatment between 24 and 96 h also suggests that light limitation may have been a factor (*SI Appendix*). Similar results were obtained in a subsequent year during the same period, whereas earlier in that year, the phytoplankton community appeared to be both iron- and cobalamin-replete. These data suggest this colimitation is a consistent, episodically important phenomenon (*SI Appendix*, Fig. S1). We examined the short-term transcriptional response of the January 16, 2013, community to cobalamin and iron addition to further characterize the nature and implications of this colimitation. RNA sequencing was performed on triplicate samples 24 h after micronutrient addition. Sequencing and assembly statistics are given in Dataset S1. This timescale is short relative to phytoplankton community growth rates (0.23 ± 0.09 d^{-1}; Chl *a*-specific growth rate). Thus, observed differences in transcript abundance are expected to directly reflect responses to changes in micronutrient availability, rather than shifts in community composition. This is supported by phylogenetic contributions to the mRNA pool, as well as 16S and 18S ribosomal RNA amplicon analyses (Fig. 1; *SI Appendix*, Figs. S2 and S3). Diatoms, particularly *Fragilariopsis* and *Pseudonitzchia*, made up the majority of the phytoplankton community (Fig. 1 *B* and *C*; *SI Appendix*, Table S1). Bacterial contributions to the mRNA pool were dominated by Proteobacteria and Bacteroidetes, with minimal archaeal or cyanobacterial contributions (Fig. 1*D*), consistent with our 16s rRNA amplicon analyses (*SI Appendix*, Fig. S3), as well as previous austral summer Southern Ocean observations (12, 13).

Across all major groups in the community, cobalamin addition drove a more extensive transcriptional shift than iron addition (*SI Appendix*, Fig. S4), suggesting diverse microbes are poised to manage and respond to cobalamin deprivation. Diatoms, the major primary producers in this system, displayed transcriptional patterns consistent with the simultaneous cobalamin and iron limitation observed via Chl *a*. Previously identified diatom cobalamin stress indicators cobalamin acquisition protein 1 (CBA1) and MetE (8, 19) were repressed by cobalamin addition across a range of diatom taxa, regardless of iron status (Fig. 2; *SI Appendix*, Figs. S5 and S6). CBA1 is involved in cobalamin acquisition (19), and its transcripts were present at 9 ± 4 × 10^7 copies·L^{-1} in control and +Fe treatments, and were repressed to 2 ± 0.4 × 10^7 copies·L^{-1} 24 h after cobalamin addition. MetE replaces the cobalamin requirement in diatoms (8) and its transcripts were repressed from 3 ± 1 × 10^8 to 6 ± 0.4 × 10^6 copies·L^{-1}. Their relatively high expression in unamended control samples thus reflected cobalamin stress in the natural community. A subset of diatom sequences encoding the canonical iron starvation indicator flavodoxin (22) were significantly repressed by iron addition, as were select transcripts encoding another diatom iron starvation-induced protein, ISIP2A (23) (Fig. 2; *SI Appendix*, Figs. S5 and S6). Multiple diatom ISIP2A and flavodoxin encoding ORFs were not repressed 24 h after iron addition. These ORFs may have been repressed by iron addition on a different timescale, or it may be that some Antarctic diatoms constitutively express these genes, as observed previously for flavodoxin (24). Nitrate uptake rates were elevated after iron addition, in line with observed up-regulation of diatom

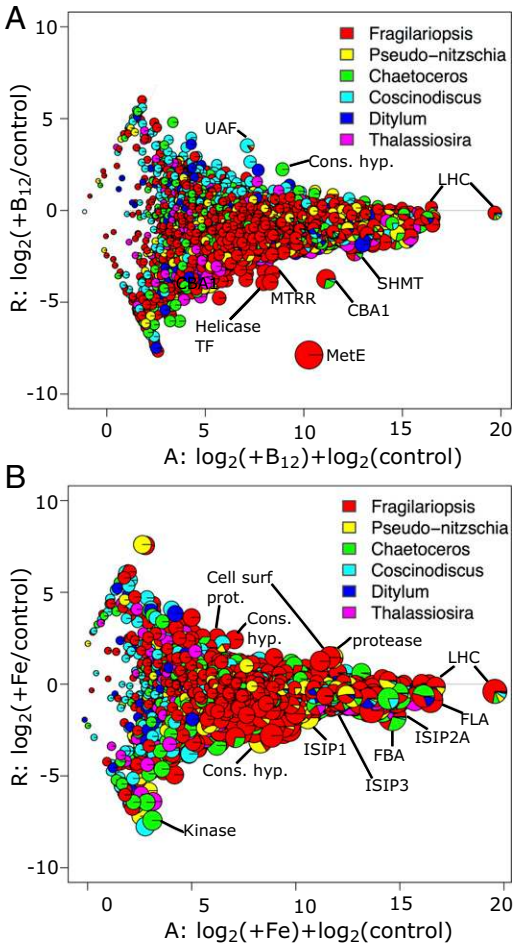

Fig. 2. Differential transcript abundance patterns in diatoms 24 h after micronutrient addition, comparing cobalamin addition versus control (*A*) and iron addition versus control (*B*) (20). Each pie represents a cluster of diatom ORFs identified using MCL (21). LPI-based phylogenies of clusters, including the top six most abundant diatom genera, are shown. Consensus annotations for clusters of interest are given. Cons. hyp, conserved hypothetical protein; flavodoxin, clade II flavodoxin; Helicase TF, helicase-like transcription factor; ISIP1, 2A, 3, iron starvation-induced proteins 1, 2A, and 3; LHC, light-harvesting complex-associated proteins; FBA, fructose bisphosphate aldolase; MetE, cobalamin-independent methionine synthase; MTRR, methionine synthase reductase; SHMT, serine hydroxymethyltransferase; UAF, RNA polymerase I upstream activation factor.

genes encoding nitrate transporters (*SI Appendix*, Fig. S7). Notably, alleviation of iron limitation was not required for this community to display signs of cobalamin stress, and vice versa, supporting the conclusion that these nutrients simultaneously limited community growth. Although it is possible that this response, along with the observed chlorophyll production pattern, could be produced if different groups within the primary producer community were limited by iron and others by cobalamin, a dominant diatom species in this experiment (*Fragilariopsis cylindrus*) was simultaneously iron- and cobalamin-deprived. CBA1, MetE, and ISIP2A sequences that showed >99–95% identity (blastp) to this genome were repressed by cobalamin and iron additions, respectively (Table 1). These observations support a model for colimitation whereby growth can be reduced as a result of deprivation of two nutrients simultaneously (25). Certain types of colimitation, such as biochemical substitution or dependent limitation (25), do not have known molecular mechanisms pertaining to iron and cobalamin in eukaryotic phytoplankton. Rather, diatom cobalamin use appears to be largely independent of iron demand and use (8), suggesting this is an instance of independent colimitation (25).

Given that cobalamin is produced only by bacteria and archaea, a full understanding of cobalamin colimitation in phytoplankton requires interrogation of these communities as well. Through combining these transcriptome data with a genome sequence obtained from the assembly of metagenomic data recovered from another Southern Ocean surface water community, we identify the *Oceanospirillaceae* ASP10-02a population as the dominant source of transcriptional capacity for cobalamin biosynthesis, contributing more than 70% of cobalamin biosynthesis-associated reads in this experiment (Fig. 3; Dataset S2). We also suggest this group is a key contributor to cobalamin biosynthesis throughout Austral summer surface waters of the Southern Ocean, as it contributes the majority of *cbiA*/*cobB* (cobyrinic acid a,c-diamide synthase) metagenomic sequences from a range of Southern Ocean locations in that season, when *Thaumarchaea* and SAR324 contributions are low (*SI Appendix*, Fig. S8). *Oceanospirillaceae* ASP10-02a also contributes a majority of CobU (adenosylcobinamide kinase)-encoding sequences in Southern Ocean metagenomes (*SI Appendix*, Fig. S8). In addition, *Oceanospirillaceae* ASP10-02a CbiA-derived peptides were previously detected in the Ross Sea [identified as Group RSB12 (15); *SI Appendix*, Fig. S9]. The assembled *Oceanospirillaceae* ASP10-02a genome also recruited nearly 20% of all bacterial-assigned reads from this experiment, suggesting it is an important contributor to this community (Fig. 3; Dataset S3). High expression levels of a diverse suite of organic compound acquisition genes, possible cell surface attachment-related genes (26), and photoheterotrophy genes were detected and attributed to *Oceanospirillaceae* ASP10-02a (*SI Appendix*, Fig. S10). This key cobalamin producer may thus have been directly associated with phytoplankton cells and acquiring a wide range of phytoplankton-derived organic compounds as growth substrates, suggesting a mutualistic relationship.

Notably, *Oceanospirillaceae* ASP10-02a-attributed cobalamin biosynthesis pathway genes did not show differential expression upon vitamin addition. However, in other bacteria, genes attributed to the final steps in the pathway (e.g., *cobU*) were repressed by cobalamin addition (Fig. 3; Dataset S2). This latter part of the pathway can be referred to as the salvage and repair portion and is present in many bacterial genomes that do not encode the entire biosynthesis pathway (27). Although *Oceanospirillaceae* ASP10-2a contributed the majority of *cobU* reads, one ORF, most similar to a different gammaproteobacterial sequence, contributed nearly 10% of *cobU* reads and was significantly repressed by cobalamin addition (Fig. 3). This suggests that during this late Austral summer experiment, a subset of bacterial groups repressed cobalamin salvage under conditions of sufficient vitamin availability; increased cobalamin concentrations appear to have resulted in reduced repair and reuse. Sequences most similar to this cobalamin- repressed *cobU* ORF are also highly represented in Southern Ocean metagenomics datasets in the Austral summer (*SI Appendix*, Fig. S8; gammaproteobacterium HTCC2134), suggesting repression of salvage and repair may be a widespread phenomenon.

Bacteria and archaea can also be important cobalamin consumers. Previous studies in the Ross Sea and other coastal marine locations suggest bacteria are able to assimilate as much

Table 1. *F. cylindrus* was simultaneously cobalamin- and iron-stressed

ORF	Protein	Blast hit % ID	FDR Fe	FDR B_{12}
262323_522_1007+	CBA1	95	1	0.06
231834_1_471+	MetE	99	1	0.005
128213_185_1513−	ISIP2A	99	0.01	0.4

ORFs shown encode proteins with 95–99% identity (ID) to *F. cylindrus* sequences. FDR (false discovery rate) for differential expression in pairwise comparisons versus the control were calculated via edgeR.

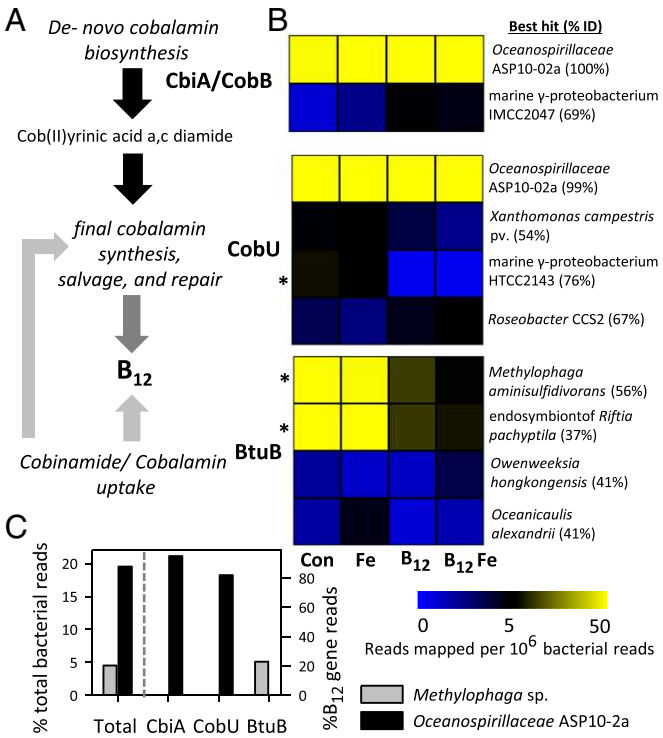

Fig. 3. *Oceanospirillaceae* ASP10-02a contributes the majority of cobalamin biosynthesis transcripts, and *Methylophaga* is an important contributor to cobalamin uptake gene expression. All ORFs attributed to cobalamin biosynthesis gene *cbiA/cobB*, cobalamin salvage, and repair gene *cobU* and cobalamin uptake gene *btuB* are shown with mean expression values in each of four treatments (*A* and *B*). Those significantly (edgeR FDR < 0.05) differentially expressed upon B_{12} addition are denoted with an asterisk. Best blast hit and percentage identity for each ORF is given. A subset of cobalamin salvage (*cobU*) and uptake (*btuB*) genes are repressed upon cobalamin addition, whereas de novo synthesis does not appear to be regulated by B_{12} availability on this timescale. Overall *Methylophaga* and *Oceanospirillaceae* ASP10-02a contributions to these transcriptomes and to *cbiA*, *cobU*, and *btuB* expression are shown in *C*. Fraction of *Methylophaga*-assigned (LPI > 0.8) reads and the fraction of reads mapping to the *Oceanospirillaceae* ASP10-2a genome (>99% identity) are shown as a percentage of total assigned bacterial-assigned (LPI > 0.8) reads. Percentage of *cbiA*, *cobU*, and *btuB* reads that we assigned to *Methylophaga* and *Oceanospirillaceae* ASP10-02a are also shown.

cobalamin as phytoplankton (14, 28). We identified four sequences encoding the bacterial cobalamin uptake protein BtuB in this study (Fig. 3). One of two highly expressed BtuB-encoding genes is most similar to those from *Methylophaga*. *Methylophaga* also contributed significantly to the total bacterial portion of the metatranscriptomes analyzed here, suggesting it may be a quantitatively important cobalamin consumer in this study (Fig. 3, Dataset S4). This group has previously been detected in other areas of the coastal Southern Ocean and across a range of additional marine locales (29–31). Characterized members of this group do not produce cobalamin (32–34), but contribute significantly to both methanol and dimethylsulfide consumption in the surface ocean (30, 31). *Methylophaga* displayed signatures of iron and cobalamin deprivation, with repressed cobalamin uptake functions upon cobalamin addition, and repressed iron complex uptake and elevated iron storage transcripts after iron addition (Fig. 4). In addition to signs of micronutrient deprivation, the *Methylophaga* group strongly expressed genes for methanol and other one-carbon compound use. These include quinoprotein methanol dehydrogenase, the enzyme required for conversion of methanol to formaldehyde, which is the initial step in assimilatory and dissimilatory methanol use (Fig. 4). Importantly, as methanol is a ubiquitous, abundant phytoplankton waste product (35), this gammaproteobacterial group also couples methanol production via phytoplankton growth to competition for cobalamin and iron.

Strong iron binding ligand production by bacteria has long been thought to play a role in enhancing iron bioavailability in the ocean (e.g., ref. 36). Here, we document repression of genes encoding siderophore uptake proteins upon iron addition, supporting the notion that siderophores are a source of iron to bacteria under iron limited conditions (Dataset S5). In addition, we document significant induction of possible bacterial siderophore biosynthesis genes upon iron addition (nonribosomal peptide biosynthesis; Dataset S5). Although counter to the canonical negative Fur regulation of siderophore production, this induction is consistent with results from iron fertilization studies,

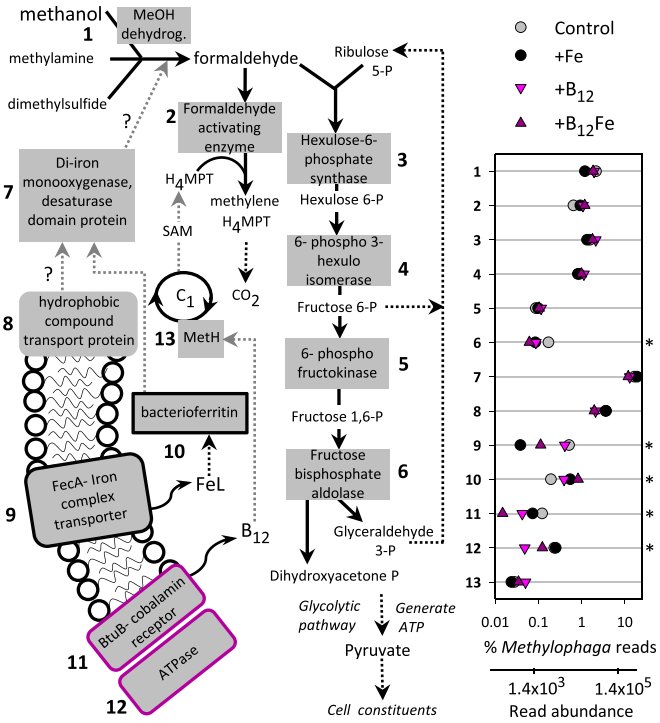

Fig. 4. Abundant ORFs assigned to *Methylophaga* and their possible connections to cobalamin and Fe responsive ORFs. Functions shown are those assigned to the 10 most abundant *Methylophaga*-assigned ORFs, other genes in the ribulose monophosphate pathway (RuMP), and select ORFs that were significantly differentially expressed between Fe or cobalamin treatments versus control. Genes encoding putative methanol dehydrogenase (1), formaldehyde-activating enzyme (2), and key enzymes in the RuMP pathway (3, 4) are among the most abundant *Methylophaga* transcripts. Multiple ORFs containing di-iron monooxygenase domains (7), as well as possible hydrophobic compound transporter domains (8), are also highly expressed. These could be involved in acquisition and metabolism of additional substrates. Functions with significantly differently expressed ORFs are highlighted in black (FDR < 0.05 control vs. +Fe) and purple (FDR < 0.05 control vs. + B_{12}) outlines and denoted with an asterisk. Among those ORFs repressed upon B_{12} addition are those encoding putative B_{12} acquisition functions (11, 12). Those significantly repressed by iron addition include FecA domain ORFs (9), likely involved in iron complex uptake. ORFs induced by iron include iron storage bacterioferritin domains (10). B_{12} quotas were possibly related to formaldehyde metabolism, as methionine synthase (MetH) (11) is required for regeneration of methylation capacity. Iron was possibly involved in formaldehyde dissimilation via a variety of ferridoxin-type oxidoreductases. Black arrows represent direct, known metabolic connections. Black dashed arrows represent known connections via multiple steps. Gray arrows represent hypothesized connections.

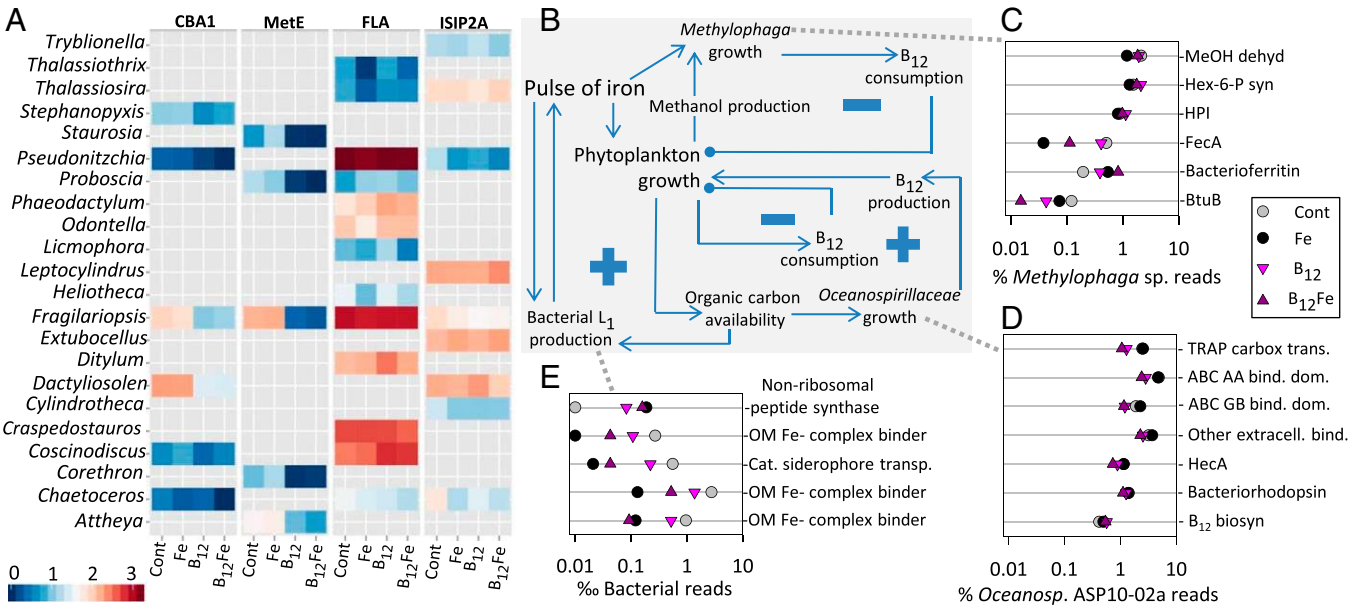

Fig. 5. A series of feedback loops, driven by phytoplankton and bacterial dynamics, appears to control interactivity of cobalamin and iron. These feedback loops are described here as responses to pulsed iron input. Molecular support for feedback loops is shown (*A*) in the heat map of relative expression levels (log10) of diatom CBA1, MetE, clade 2 flavodoxin, and ISIP2A transcripts. Bacterial gene expression patterns supporting these feedback loops include (*B*) *Methylophaga* sp. methanol consumption (methanol dehydrogenase and key ribulose monophosphate pathway enzymes) and iron and cobalamin deprivation [iron acquisition (FecA), iron storage (bacterioferritin), and cobalamin uptake (BtuB)]-related genes (*C*). Highly expressed *Oceanospirillaceae* ASP10-02a (*D*) organic matter transport and binding functions and possible adhesion functions (HecA family), as well as cobalamin biosynthesis, also support this model. Siderophore-related genes that were influenced (significant; FDR < 0.05) by iron are shown, highlighting induction of possible Bacteriodetes-associated nonribosomal peptide synthase genes by iron addition (*E*) and repression of various proteobacterial Fe-complex uptake-related genes (details provided in Dataset S5).

which have shown that iron additions may stimulate production of strong iron binding ligands in the ocean (36, 37).

A series of feedback loops driven by phytoplankton-bacterial interactions thus appear to govern coupling of cobalamin and iron dynamics in this late Austral summer system (Fig. 5). When iron is added to the system, for instance, as a result of pulsed aeolian input or melting sea ice, this will stimulate iron-limited phytoplankton growth. Availability of such iron may be enhanced as a result of bacterial ligand production, which is stimulated both by iron addition via a regulated response and, in a positive feedback loop, enhanced availability of phytoplankton- derived organic matter. Elevated phytoplankton-derived organic matter availability to bacteria is expected upon alleviation of iron limitation (38, 39). In another positive feedback loop, cobalamin production increases, also as a result of this enhanced organic matter availability, providing a mechanism for further increasing phytoplankton growth. This may be counterbalanced by negative feedback loops in which phytoplankton and bacterial demand for cobalamin increase while bacterial salvage and repair of degraded cobalamin is reduced in response to increases in cobalamin supply (Figs. 3 and 5).

In this experiment, cobalamin and iron addition alone each stimulated production, but together did not enhance Chl *a* beyond the level of iron addition alone [described as subadditive-independent colimitation (40)]. This suggests that, by 96 h, in situ cobalamin production may have been enhanced by iron addition, and a manipulative cobalamin addition was not required to generate cobalamin-replete conditions (Fig. 1; *SI Appendix*, Fig. S1). This interpretation suggests the positive feedback loop (Fig. 5) may have dominated. Alternatively, it is possible that another nutrient may have become limiting (e.g., manganese), preventing an additive effect. In contrast, previous summertime observations in the Ross Sea (5) documented a condition in which simultaneous cobalamin and iron addition stimulated substantial additional growth beyond iron addition alone [serial limitation (40)]. In this instance, it appears that the negative feedback loops offset the positive, and upon iron addition, cobalamin demand was stimulated beyond production. Each of these types of colimitation (subadditive independent and serial) have been observed repeatedly in marine, terrestrial, and freshwater systems for major nutrients (40). The results described here offer potential mechanisms that underpin microbial interactions and possibly drive this system into one type of colimitation over another. In addition, the potential light limitation observed here (Fig. 1) could also interact with the described colimitation, for instance, by altering abiotic cobalamin degradation rates or influencing iron quotas, and warrants further investigation in future efforts.

Future work is also required to understand relative rates of the processes identified here, as well as controls on when and where the positive or negative feedback loops described prevail. However, mechanisms by which bacterial community composition could substantially influence the net balance are apparent. It is also likely, given the highly seasonal nature of Southern Ocean microbial communities (12), that other important interactions may be at play during different times of year. It is clear, however, that late summer phytoplankton growth in this productive region is synergistically influenced by the availability of cobalamin and iron, which appears to be largely regulated by the interactions described here. We propose the term "interactive colimitation" to describe such scenarios, in which multiple limiting nutrient cycles are affected by one another through interactions among different microbial functional groups. This example of interactive colimitation was identified because of our relatively extensive understanding of the molecular mechanisms governing acquisition and management of these micronutrients. As studies of mutualism and competition between microbial groups advance, we anticipate that additional instances of such interactive colimitation may be identified as important drivers of marine biogeochemical processes.

Materials and Methods

On January 16, 2013, seawater was collected from 3 m depth at the sea ice edge in McMurdo Sound of the Ross Sea (77° 36.999′ S 165° 28.464′ E), using trace metal clean technique. Triplicate bottles (2.7 L) of each treatment (unamended control, + 1 nM added $FeCl_3$, + 200 pM added cyanocobalamin, and + 200 pM cyanocobalamin and 1 nM Fe) were placed in an indoor incubator at 0 °C, ~45 μmol photons $m^{-2}{\cdot}s^{-1}$ of constant light. After 24 h, RNA samples were collected (450 mL) and nitrate uptake and primary productivity rates were measured. Samples were taken for Chl *a* at 0, 24, and 96 h. RNA was extracted using the TRIzol reagent (Life Technologies). Ribosomal RNA was removed with Ribo-Zero Magnetic kits, and the resulting mRNA enrichment was purified and subjected to amplification and cDNA synthesis, using the Ovation RNA-Seq System V2 (NuGEN). One microgram of the resulting high-quality cDNA pool was fragmented to a mean length of 200 bp, and Truseq (Illumina) libraries were prepared and subjected to paired-end sequencing via Illumina HiSeq. Reads were trimmed and filtered, contigs were assembled in CLC Assembly Cell (CLCbio), and ORFs were predicted (41). ORFs were annotated de novo for function via KEGG, KO, KOG, Pfam, and TigrFam assignments. Taxonomic classification was assigned to each ORF using a reference dataset, as described in the *SI Appendix*, and the Lineage Probability Index (LPI, as calculated in ref. 18). edgeR was used to assign normalized fold change and determine which ORFs were significantly differentially expressed in pairwise comparisons between treatments, considering triplicates, within a given phylogenetic grouping (42). For Fig. 2, diatom ORFs [identified as diatom via LPI analyses; LPI > 0.8 (18)] were clustered using MCL (Markov cluster algorithm) (21), and these clusters were used to produce MANTA plots (20). For *Oceanospirillaceae* ASP10-02a genome assembly, water was collected from 10 m in the Amundsen Sea on December 19, 2010. Metagenomic libraries were created with the OVATION ultralow kit (NuGen). Overlapping and gapped metagenomic DNA libraries were prepared for sequencing on a HiSeq platform (Illumina). CLC was used to assemble scaffolds, tetranucleotide frequencies of scaffolds were analyzed (43), and draft genomes were generated via binning scaffolds clustered (hierarchical) together in well-supported clades, refined using GC content and taxonomical affiliation (44). ORFs identified in metatranscriptomic analyses were mapped to the *Oceanospirillaceae* ASP10-02a genome bin from the best-scoring nucleotide alignment, using BWA-MEM with default parameters (45). ORFs with >99% similarity to the genome scaffold sequences were used for subsequent analyses of gene expression patterns within this population. Complete materials and methods are given in the *SI Appendix*.

ACKNOWLEDGMENTS. We thank Nathan Walworth and Ariel Rabines for assistance in the laboratory and field and Rob Middag for iron concentration measurements in our cobalamin stock. We are grateful to Antarctic Support Contractors, especially Jen Erxleben and Ned Corkran, for facilitating fieldwork and to Mak Saito for helpful comments on the manuscript. This study was funded by National Science Foundation (NSF) Antarctic Sciences Awards 1103503 (to E.M.B.), 0732822 and 1043671 (to A.E.A.), 1043748 (to D.A.H.), 1043635 (to D.A.B.), and 1142095 (to A.F.P.); Gordon and Betty Moore Foundation Grant GBMF3828 (to A.E.A.); and NSF Ocean Sciences Award 1136477 (to A.E.A.).

1. Arrigo KR, et al. (1999) Phytoplankton community structure and the drawdown of nutrients and CO_2 in the southern ocean. *Science* 283(5400):365–367.
2. Matsumoto K, Sarmiento JL, Brzezinski M (2002) Silicic acid leakage from the Southern Ocean: A possible explanation for glacial atmospheric pCO_2. *Global Biogeochem Cycles* 16((3):5-1–5-3.
3. Arrigo KR, van Dijken GL, Bushinsky S (2008) Primary production in the Southern Ocean, 1997–2006. *JGR Oceans* 113(C8):C08004.
4. Martin JH, Fitzwater SE, Gordon RM (1990) Iron deficiency limits plankton growth in Antarctic waters. *Global Biogeochem Cycles* 4:5–12.
5. Bertrand EM, et al. (2007) Vitamin B_{12} and iron co-limitation of phytoplankton growth in the Ross Sea. *Limnol Oceanogr* 52(3):1079–1093.
6. Panzeca C, et al. (2006) B vitamins as regulators of phytoplankton dynamics. *Eos* 87(52):593–596.
7. Croft MT, Lawrence AD, Raux-Deery E, Warren MJ, Smith AG (2005) Algae acquire vitamin B_{12} through a symbiotic relationship with bacteria. *Nature* 438(7064):90–93.
8. Bertrand EM, et al. (2013) Methionine synthase interreplacement in diatom cultures and communities: Implications for the persistence of B_{12} use by eukaryotic phytoplankton. *Limnol Oceanogr* 58(4):1431–1450.
9. Doxey AC, Kurtz DA, Lynch M, Sauder LA, Neufeld JD (2015) Aquatic metagenomes implicate Thaumarchaeota in global cobalamin production. *ISME J* 9(2):461–471.
10. Bonnet S, et al. (2010) Vitamin B_{12} excretion by cultures of the marine cyanobacteria *Crocosphaera* and *Synechococcus*. *Limnol Oceanogr* 55(5):1959–1964.
11. Marchant HJ (2005) Cyanophytes. *Antarctic Marine Protists*, eds Scott FJ, Marchant HJ (Australian Biological Resources Study, Canberra), pp 324–325.
12. Wilkins D, et al. (2013) Key microbial drivers in Antarctic aquatic environments. *FEMS Microbiol Rev* 37(3):303–335.
13. Williams TJ, et al. (2012) A metaproteomic assessment of winter and summer bacterioplankton from Antarctic Peninsula coastal surface waters. *ISME J* 6(10):1883–1900.
14. Bertrand EM, et al. (2011) Iron limitation of a springtime bacterial and phytoplankton community in the ross sea: Implications for vitamin b($_{12}$) nutrition. *Front Microbiol* 2:160.
15. Bertrand EM, Saito MA, Jeon YJ, Neilan BA (2011) Vitamin B_{12} biosynthesis gene diversity in the Ross Sea: The identification of a new group of putative polar B_{12} biosynthesizers. *Environ Microbiol* 13(5):1285–1298.
16. Kazamia E, et al. (2012) Mutualistic interactions between vitamin B12 -dependent algae and heterotrophic bacteria exhibit regulation. *Environ Microbiol* 14(6):1466–1476.
17. Rivkin R (1991) Seasonal Patterns of Planktonic Production in McMurdo Sound, Antarctica. *Am Zool* 31(1):5–16.
18. Podell S, Gaasterland T (2007) DarkHorse: A method for genome-wide prediction of horizontal gene transfer. *Genome Biol* 8(2):R16.
19. Bertrand EM, et al. (2012) Influence of cobalamin scarcity on diatom molecular physiology and identification of a cobalamin acquisition protein. *Proc Natl Acad Sci USA* 109(26):E1762–E1771.
20. Marchetti A, et al. (2012) Comparative metatranscriptomics identifies molecular bases for the physiological responses of phytoplankton to varying iron availability. *Proc Natl Acad Sci USA* 109(6):E317–E325.
21. van Dongen S (2000) A cluster algorithm for graphs. Technical Report INS-R0010. (National Research Institute for Mathematics and Computer Science in the Netherlands, Amsterdam).
22. LaRoche J, Boyd PW, McKay RM, Geider RJ (1996) Flavodoxin as an in situ marker for iron stress in phytoplankton. *Nature* 382:802–805.
23. Allen AE, et al. (2008) Whole-cell response of the pennate diatom *Phaeodactylum tricornutum* to iron starvation. *Proc Natl Acad Sci USA* 105(30):10438–10443.
24. Pankowski A, McMinn A (2009) Development of imunoassays for the iron-regualted proteins ferredoxin and flavodoxin in polar microalgae. *J Phycol* 45(3):771–783.
25. Saito MA, Goepfert TJ, Ritt JT (2008) Some thoughts on the concept of co-limitation: Three definitions and the importance of bioavailability. *Limnol Oceanogr* 53(1):276–290.
26. Rojas CM, Ham JH, Deng WL, Doyle JJ, Collmer A (2002) HecA, a member of a class of adhesins produced by diverse pathogenic bacteria, contributes to the attachment, aggregation, epidermal cell killing, and virulence phenotypes of *Erwinia chrysanthemi* EC16 on *Nicotiana clevelandii* seedlings. *Proc Natl Acad Sci USA* 99(20):13142–13147.
27. Rodionov DA, Vitreschak AG, Mironov AA, Gelfand MS (2003) Comparative genomics of the vitamin B_{12} metabolism and regulation in prokaryotes. *J Biol Chem* 278(42):41148–41159.
28. Koch F, et al. (2011) The effect of vitamin B_{12} on phytoplankton growth and community structure in the Gulf of Alaska. *Limnolog Oceanog* 56(3):1023–1034.
29. Grzymski JJ, et al. (2012) A metagenomic assessment of winter and summer bacterioplankton from Antarctica Peninsula coastal surface waters. *ISME J* 6(10):1901–1915.
30. Neufeld JD, Boden R, Moussard H, Schäfer H, Murrell JC (2008) Substrate-specific clades of active marine methylotrophs associated with a phytoplankton bloom in a temperate coastal environment. *Appl Environ Microbiol* 74(23):7321–7328.
31. Vila-Costa M, et al. (2006) Phylogenetic identification and metabolism of marine dimethylsulfide-consuming bacteria. *Environ Microbiol* 8(12):2189–2200.
32. Boden R, Kelly DP, Murrell JC, Schäfer H (2010) Oxidation of dimethylsulfide to tetrathionate by *Methylophaga thiooxidans* sp. nov.: A new link in the sulfur cycle. *Environ Microbiol* 12(10):2688–2699.
33. Villeneuve C, Martineau C, Mauffrey F, Villemur R (2012) Complete genome sequences of *Methylophaga* sp. strain JAM1 and *Methylophaga* sp. strain JAM7. *J Bacteriol* 194(15):4126–4127.
34. Kim HG, Doronina NV, Trotsenko YA, Kim SW (2007) *Methylophaga aminisulfidivorans* sp. nov., a restricted facultatively methylotrophic marine bacterium. *Int J Syst Evol Microbiol* 57(Pt 9):2096–2101.
35. Dixon JL, Beale R, Nightingale PD (2013) Production of methanol, acetaldehyde, and acetone in the Atlantic Ocean. *Geophys Res Lett* 40(17):4700–4705.
36. Rue EL, Bruland KW (1997) The role of organic complexation on ambient iron chemistry in the equatorial Pacific Ocean and the response of a mesoscale iron addition experiment. *Limnol Oceanogr* 42(5):901–910.
37. Kondo Y, et al. (2008) Organic iron(III) complexing ligands during an iron enrichment experiment in the western subarctic North Pacific. *Geophys Res Lett* 35(12):L12601.
38. Bequevort S, Lancelot C, Schoemann V (2007) The role of iron in bacterial degradation of organic matter derived from *Phaeocystis antarctica*. *Biogeochemistry* 83:119–135.
39. Rochelle-Newall EJ, Ridame C, Dimier-Hugueney C, L'Helguen S (2014) Impact of iron limitation on primary production (dissolved and particulate) and secondary production in cultured Trichodesmium sp. *Aquat Microb Ecol* 72(2):143–153.
40. Harpole WS, et al. (2011) Nutrient co-limitation of primary producer communities. *Ecol Lett* 14(9):852–862.
41. Rho M, Tang H, Ye Y (2010) FragGeneScan: Predicting genes in short and error-prone reads. *Nucleic Acids Res* 38(20):e191.
42. Robinson MD, McCarthy DJ, Smyth GK (2010) edgeR: A Bioconductor package for differential expression analysis of digital gene expression data. *Bioinformatics* 26(1):139–140.
43. Ihaka R, Gentleman R (1996) R: A language for data analysis and graphics. *J Comput Graph Stat* 5:299–314.
44. Brady A, Salzberg SL (2009) Phymm and PhymmBL: Metagenomic phylogenetic classification with interpolated Markov models. *Nat Methods* 6(9):673–676.
45. Li H (2013) Aligning sequence reads, clone sequences and assembly contigs with BWA-MEM. arXiv:1303.3997.